

Operator Fitting for Parameter Estimation of Stochastic Differential Equations

ASBJØRN N. RISETH* AND JAKE P. TAYLOR-KING*†

Abstract. Estimation of parameters is a crucial part of model development. When models are deterministic, one can minimise the fitting error; for stochastic systems one must be more careful. Broadly, parameterisation methods for stochastic dynamical systems fit into maximum likelihood estimation- and method of moment-inspired techniques. We propose a method where one matches a finite dimensional approximation of the Koopman operator with the implied Koopman operator as generated by an extended dynamic mode decomposition approximation. One advantage of this approach is that the objective evaluation cost can be independent the number of samples for many dynamical systems. We test our approach on two simple systems in the form of stochastic differential equations, compare to benchmark techniques, and consider limited eigen-expansions of the operators being approximated. Other small variations on the technique are also considered, and we discuss the advantages to our formulation.

Key words. Extended Dynamic Mode Decomposition, EDMD, Stochastic Differential Equations, SDEs, Parameter Estimation, Parameter Inference, Koopman Operator, Transition Operator, Infinitesimal Generator.

1. Introduction. In multiple application areas, such as physics and biology, noise plays an important role in the system dynamics [5, 32]. One way to include noise into the dynamics is to add suitable stochastic terms to ordinary differential equations (ODEs), which leads to so-called stochastic differential equations (SDEs) [24]. Possible dynamics of SDEs compared to ODEs are then greatly enriched due to the presence of noise, making the SDE suitable to capture intriguing noise-induced phenomena, such as noise-induced switching, oscillations, and focusing [4, 5, 32].

With a family of parameterised deterministic dynamical systems, one typically chooses parameters such that a suitable objective function is minimised. In the case of continuous state-space dynamical systems, usually one minimises the mean squared error between model prediction and observed data; this can be achieved via nonlinear least squares [2, 25, 28]. However, methods useful in the deterministic setting are unsuitable when applied to dynamical systems with intrinsic noise — especially when noise-induced phenomena are present.

Many well behaved dynamical systems have an associated forward and backward interpretation [14, 15]. Depending on the interpretation used, this can lead to different numerical methods for parameter estimation [10, 12]. The forward interpretation describes the time-evolution of the probability that the system is in some state, and is known as the Perron–Frobenius operator (PFO). The PFO naturally links to maximum likelihood estimation (MLE), where one selects parameters for a model such that the probability of observed data being realised (by said model) is maximised. The backward interpretation is adjoint to the forward interpretation and describes the time-evolution of expectations, known as the Koopman¹ operator (KO). In the method of moments (MM), parameters are chosen to match theoretical expected values of a model to sample mean values as calculated from an observed data set. Naturally, solving the

*Mathematical Institute, University of Oxford, Oxford, OX2 6GG, UK

†Department of Integrated Mathematical Oncology, H. Lee Moffitt Cancer Center and Research Institute, Tampa, FL, USA

Contact email: taylor-king@imso.biol.ethz.ch

¹ The Koopman operator for random dynamical systems is also called the stochastic Koopman operator, or, in probability terminology, the transition operator.

PFO or KO via numerical scheme and implementing a minimisation procedure to find the optimal parameter choice can be computationally intensive, so various methods have been proposed, for example, Monte Carlo simulation, or approximate Bayesian computation [6, 11, 27].

Recently, using data to numerically reconstruct the Koopman operator and the Perron–Frobenius operator (and their eigendecompositions) have become a popular area of study [14, 15]. One of these methods is known as Extended Dynamic Mode Decomposition (EDMD) [18, 33], which uses basis functions to project the data into a higher dimensional space, where it is assumed dynamics are linear. Therefore one can propagate forward nonlinear models in a linear fashion. Depending on the basis functions used, EDMD methods can scale very well with dimension and efficient numerical schemes have been proposed. For example, Williams *et. al.* [29] used an Arnoldi type algorithm for analysing data from direct numerical simulations of a turbulent flow on a $256 \times 201 \times 144$ grid, and Tu *et. al.* [31] presented a SVD based algorithm that was applied to analysis of an incompressible Navier–Stokes generated flow on a 1500×500 grid.

To avoid the limitless possible stochastic dynamical systems we could consider, we restrict ourselves to SDEs. In the case of SDEs, the PFO defines the Fokker–Planck equation and the KO defines the Kolmogorov backward equation. In the review by Hurn *et. al.* [12], two classification terms were identified as alternatives to exact MLE². These were: likelihood based procedures, essentially trying to estimate the likelihood function using a numerical scheme; and the obscurely named “sample DNA matching” procedures, where one tries to match some feature(s) of the model to some feature(s) of the data — essentially accounting for all other parameter estimation methods.

Our method involves the following steps: we calculate the EDMD matrix as implied by the data; we use the same basis functions as the EDMD matrix to build a matrix representation of the Koopman operator; and we then choose parameters such that these matrices are as close as possible (under some norm). We prove that, under relevant conditions, EDMD estimates the correct Koopman operator with a mean-square error that scales with the inverse of the number of data points. A similar approach of matching matrix representations of operators within the Koopman framework have also been proposed in [20, 21], where they focus on ODEs with polynomial nonlinearities. Numerical tests indicate convergence of the root mean squared error as the amount of data increases. Fundamental to EDMD is that one can decompose the (approximate) Koopman operator into eigenfunctions. For one of our numerical examples we use this idea to show that for large quantities of data, a limited eigen-expansion can provide better parameter estimates when compared to the full matrix representation. Our method is neither an MLE based method nor an MM based method, but can be placed in the category of sample DNA matching methods as described by Hurn *et. al.* [12].

Using our EDMD-based approach, we can carry out computationally cheap parameterisations of SDEs (depending on the choice in basis functions). Our method is comparable to other standard techniques for SDEs, and we also mention variations on our method. The method is general in that it should be clear how to adapt the approach to other dynamical systems.

The paper is organised as follows. Our algorithm and its theoretical motivation are in [Section 2](#), and numerical experiments are in [Section 3](#). We consider variations

²Exact MLE was the term used to describe the case where the transition probability had a known analytic expression.

of our algorithm and similarities to existing methods in [Section 4](#), and discuss further work in [Section 5](#).

2. Markov operators of SDEs. We are concerned with parameter estimation for one-dimensional autonomous SDEs of the form³

$$(1) \quad dX_t = a(X_t; \theta) dt + b(X_t; \theta) dW_t.$$

Here, W_t is a standard Brownian motion, and $a(x; \theta)$ and $b(x; \theta)$ are drift and volatility functions parameterised by θ from some parameter set Θ . To the SDE (1) there is an associated transition operator semigroup that describe the expected evolution of functions of the state. We follow the DMD-literature and refer to these operators as Koopman operators, due to [\[16, 19\]](#). For our purposes, assume that $a(x; \theta)$ and $b(x; \theta)$ are well behaved, so that a strong solution to the SDE exists for relevant initial conditions. Given a data set, believed to be generated by a process of the form (1), we want to obtain a parameter estimate $\hat{\theta}$. When using synthetic data generated by the SDE with parameter θ^* , we wish for our estimate to match the true value.

Our approach builds on Koopman theory and EDMD to find $\hat{\theta}$. The core idea of the proposed algorithm is to compare an EDMD operator, approximated from data, with the Koopman operator associated with (1). We can also place the Perron–Frobenius operator in the context of our algorithm; however, as EDMD is best understood as an approximation to the Koopman operator we focus on the backward interpretation (with occasional mentions to the forward interpretation). We start by introducing the relevant theory, before formalising our algorithm. The contents of [Subsections 2.2](#) and [2.3](#) follows the exposition of Korda and Mezić [\[17\]](#).

2.1. The Koopman Operator. Denote by $\mathcal{M} \subset \mathbb{R}$ the state space of the SDE (1). Define X_t^x to be the solution to the SDE at time t , with initial condition $X_0 = x$.

DEFINITION 2.1. *The time $t \geq 0$ Koopman operator on functions $g : \mathcal{M} \rightarrow \mathbb{R}$, is given by*

$$(2) \quad \mathcal{K}^t g(x) = \mathbb{E}_W [g(X_t^x)],$$

where the expectation is taken with respect to the paths of the Brownian motion W_t .

We require that the domain of \mathcal{K}^t is such that $g(X_t^x)$ is integrable with respect to the paths of the Brownian motion. Note that \mathcal{K}^t is linear on the space of functions. In the case of an ODE, that is, when $b(x; \theta) \equiv 0$, the solution X_t^x is deterministic and the Koopman operator is just $\mathcal{K}^t g(x) = g(X_t^x)$.

For completeness we note that the Perron–Frobenius operator can be viewed as the adjoint of the Koopman operator. Associate a probability space $(\mathcal{M}, \mathcal{B}, \mu)$ to the state space of the SDE (1). The operators are then adjoint under the duality pairing between $L^1(\mathcal{M}, \mu)$ and $L^\infty(\mathcal{M}, \mu)$, the spaces of integrable, and essentially bounded functions respectively. See, for example Klus *et. al.* [\[14\]](#), for a broader discussion of the duality between the two operators and their numerical approximations.

2.2. Extended Dynamic Mode Decomposition. Suppose we are given snapshots of input-output data

$$(3) \quad \mathbf{X} = [x_1, \dots, x_T], \quad \mathbf{Y} = [y_1, \dots, y_T],$$

³In this paper, we only consider one-dimensional SDEs, although higher dimensional SDEs follow naturally.

where y_j is a realisation of $X_t^{x_j}$ for some fixed time-step $t > 0$. If the data is a sample path of the solution to the SDE, we have that $x_{j+1} = y_j$ for $j = 1, \dots, T-1$, that is, $x_{j+1} = X_{j+1}^{x_1}$. In the remainder of the manuscript we either assume that the data points x_j are drawn independently from a given distribution μ , or from the Markov chain $x_{j+1} = X_t^{x_j}$, started at a known point $x_1 \in \mathcal{M}$. Some convergence properties are guaranteed if the Markov chain is Ergodic [17].

The EDMD procedure for characterising the dynamical system that generated the data starts with a choice of linearly independent functions $\psi_j : \mathcal{M} \rightarrow \mathbb{R}$, $j = 1, \dots, N$. By first defining the vector field $\boldsymbol{\psi} : \mathcal{M} \rightarrow \mathbb{R}^N$ as

$$(4) \quad \boldsymbol{\psi}(x) = [\psi_1(x), \dots, \psi_N(x)]^\top,$$

we specify the matrices $\boldsymbol{\psi}(\mathbf{X}), \boldsymbol{\psi}(\mathbf{Y}) \in \mathbb{R}^{N \times T}$ as

$$(5) \quad \boldsymbol{\psi}(\mathbf{X}) = [\boldsymbol{\psi}(x_1), \dots, \boldsymbol{\psi}(x_T)], \quad \boldsymbol{\psi}(\mathbf{Y}) = [\boldsymbol{\psi}(y_1), \dots, \boldsymbol{\psi}(y_T)].$$

Given the basis functions and the data, we solve the linear least squares problem

$$(6) \quad \min_{A \in \mathbb{R}^{N \times N}} \|A\boldsymbol{\psi}(\mathbf{X}) - \boldsymbol{\psi}(\mathbf{Y})\|_F^2 = \min_{A \in \mathbb{R}^{N \times N}} \sum_{j=1}^T \|A\boldsymbol{\psi}(x_j) - \boldsymbol{\psi}(y_j)\|_2^2.$$

The map $\|A\|_F^2 := \sum_{i=1}^N \sum_{j=1}^N |A_{i,j}|^2$ is known as the Frobenius norm. Let A^\dagger denote the Moore-Penrose pseudo-inverse of a matrix A [26]. A solution to the minimisation is given by

$$(7) \quad \begin{aligned} \hat{A}_T &= \boldsymbol{\psi}(\mathbf{Y})\boldsymbol{\psi}(\mathbf{X})^\dagger \\ &= \boldsymbol{\psi}(\mathbf{Y})\boldsymbol{\psi}(\mathbf{X})^\top (\boldsymbol{\psi}(\mathbf{X})\boldsymbol{\psi}(\mathbf{X})^\top)^{-1}, \end{aligned}$$

where the second equality holds so long as the rows of $\boldsymbol{\psi}(\mathbf{X})$ are linearly independent. Using the EDMD matrix, one can construct a linear operator that approximately characterises the evolution of functions under the dynamical system that generated the data.

DEFINITION 2.2. *Let $G_\boldsymbol{\psi}$ be the linear span of the functions ψ_1, \dots, ψ_N . Define the time $t \geq 0$ EDMD operator $\hat{\mathcal{K}}_T^t : G_\boldsymbol{\psi} \rightarrow G_\boldsymbol{\psi}$ on functions $g(x) = c_g^\top \boldsymbol{\psi}(x)$, with $c_g \in \mathbb{R}^N$, by*

$$(8) \quad \hat{\mathcal{K}}_T^t g(x) = c_g^\top \hat{A}_T \boldsymbol{\psi}(x).$$

2.3. Connection between Koopman and EDMD operators. The EDMD operator approximates the projection of the Koopman operator onto $G_\boldsymbol{\psi}$, with respect to a data-driven inner product. Assume that there exists a subspace of $L^2(\mathcal{M}, \mu)$ that is invariant under \mathcal{K}^t for all $t \geq 0$, and denote the largest such space by \mathcal{G} . We will henceforth consider the Koopman operators $\mathcal{K}^t : \mathcal{G} \rightarrow \mathcal{G}$. Assume that the basis functions ψ_j belong to \mathcal{G} for $j = 1, \dots, N$, so that $G_\boldsymbol{\psi} \leq \mathcal{G}$. The $L^2(\mu)$ projection onto $G_\boldsymbol{\psi}$ is defined as

$$(9) \quad P_\boldsymbol{\psi}^\mu g = \arg \min_{f \in G_\boldsymbol{\psi}} \int_{\mathcal{M}} (f - g)^2 d\mu = \boldsymbol{\psi}^\top \arg \min_{c \in \mathbb{R}^N} \int_{\mathcal{M}} (c^\top \boldsymbol{\psi} - g)^2 d\mu.$$

As $G_\boldsymbol{\psi}$ is finite-dimensional, the projected Koopman operator $\mathcal{K}_\mu^t : G_\boldsymbol{\psi} \rightarrow G_\boldsymbol{\psi}$ defined by $\mathcal{K}_\mu^t = P_\boldsymbol{\psi}^\mu \mathcal{K}^t$ has an associated matrix representation. This matrix can be written

as $A_\mu = K_\mu M_\mu^{-1}$, where

$$(10) \quad M_\mu = \int_{\mathcal{M}} \boldsymbol{\psi} \boldsymbol{\psi}^\top d\mu, \quad K_\mu = \int_{\mathcal{M}} (\mathcal{K}^t \boldsymbol{\psi}) \boldsymbol{\psi}^\top d\mu.$$

The matrix M_μ is often referred to as the mass matrix, or the Gramian matrix. The next result and subsequent proof is adapted from [17].

THEOREM 2.3. *If the matrix M_μ is invertible, then for $g = c_g^\top \boldsymbol{\psi} \in G_\psi$ we have*

$$(11) \quad \mathcal{K}_\mu^t g = c_g^\top A_\mu \boldsymbol{\psi}.$$

Proof. By the definition of the projection operator,

$$(12) \quad P_\psi^\mu \mathcal{K}^t g = \boldsymbol{\psi}^\top \arg \min_{c \in \mathbb{R}^N} \int_{\mathcal{M}} [c^\top \boldsymbol{\psi} - c_g^\top (\mathcal{K}^t \boldsymbol{\psi})]^2 d\mu$$

$$(13) \quad = \boldsymbol{\psi}^\top \arg \min_{c \in \mathbb{R}^N} [c^\top M_\mu c - 2c^\top K_\mu^\top c_g].$$

The minimiser is unique, and is given by $c = M_\mu^{-1} K_\mu^\top c_g$. It therefore follows that

$$(14) \quad \mathcal{K}_\mu^t g = c^\top \boldsymbol{\psi} = c_g^\top K_\mu M_\mu^{-1} \boldsymbol{\psi} = c_g^\top A_\mu \boldsymbol{\psi}. \quad \square$$

For the rest of the article, we assume that M_μ is invertible.

Define the data-driven measure μ_T from the input data, so that

$$(15) \quad \mu_T(x) = \frac{1}{T} \sum_{j=1}^T \delta(x - x_j),$$

where $\delta(x)$ is the Dirac delta function. For data coming from a deterministic dynamical system, such as an ODE, we show that the EDMD-operator is equal to the $L^2(\mu_T)$ -projection of \mathcal{K}^t . Further, we provide evidence for why the EDMD operator is also a reasonable estimator in the SDE case.

PROPOSITION 2.4. *If the system is deterministic, that is, $b(x; \theta) \equiv 0$, then the projected Koopman operator $\mathcal{K}_{\mu_T}^t = P_\psi^{\mu_T} \mathcal{K}^t$ is equal to the EDMD operator $\hat{\mathcal{K}}_T$:*

$$(16) \quad \mathcal{K}_{\mu_T}^t g = \hat{\mathcal{K}}_T g, \quad \forall g \in G_\psi.$$

Proof. We prove the equivalence of the finite-dimensional, linear operators by showing that their matrix representations are equal. Remember that the EDMD matrix is given by

$$\hat{A}_T = \boldsymbol{\psi}(\mathbf{Y}) \boldsymbol{\psi}(\mathbf{X})^\top (\boldsymbol{\psi}(\mathbf{X}) \boldsymbol{\psi}(\mathbf{X})^\top)^{-1}.$$

Under the empirical measure μ_T , we have that

$$(17) \quad M_{\mu_T} = \int_{\mathcal{M}} \boldsymbol{\psi}(x) \boldsymbol{\psi}(x)^\top d\mu_T(x) = \frac{1}{T} (\boldsymbol{\psi}(\mathbf{X}) \boldsymbol{\psi}(\mathbf{X})^\top).$$

Also, note that for data pairs (x_j, y_j) coming from a deterministic system,

$$(18) \quad \mathcal{K}^t g(x_j) = \mathbb{E}_W[g(X_t^{x_j})] = g(y_j).$$

In the same fashion as for the mass matrix, the empirical measure then implies that

$$(19) \quad K_{\mu_T} = \frac{1}{T} ((\mathcal{K}^t \boldsymbol{\psi}(\mathbf{X})) \boldsymbol{\psi}(\mathbf{X})^\top) = \frac{1}{T} (\boldsymbol{\psi}(\mathbf{Y}) \boldsymbol{\psi}(\mathbf{X})^\top).$$

Thus, the result follows since $A_{\mu_T} = K_{\mu_T} M_{\mu_T}^{-1} = \hat{A}_T$. \square

The proof of [Proposition 2.4](#) indicates that the EDMD operator approximates the projected Koopman operator for an SDE. The approximation error arises when approximating K_{μ_T} with \hat{K}_T , by replacing $\mathcal{K}^t \psi(x_j) = \mathbb{E}_W [\psi(X_t^{x_j})]$ with $\psi(y_j)$. The proposed algorithm in the next section is based on matching the Frobenius norm of the matrix representation of operators, and we shall thus discuss how well the EDMD matrix approximates the projected Koopman operator matrix. To start, we show that the matrix \hat{K}_T is an unbiased estimator of K_{μ_T} with variance of the order $\mathcal{O}(T^{-1})$. To show this we must first make some assumptions on the second-order moments arising from the SDE and the sampling of the x_j .

ASSUMPTION 2.5. *For a fixed $t > 0$, let the data $(x_j)_{j=1}^T$ be drawn either independently from a probability measure μ , or from a Markov chain $x_{j+1} = X_t^{x_j}$, started at a known point $x_1 \in \mathcal{M}$. Let $f, g \in \{\psi_1, \dots, \psi_N\}$. Assume that there exists a $\tilde{\gamma} > 0$ that satisfies the following.*

In the case when the x_j are i.i.d. drawn from μ ,

$$(20) \quad \mathbb{E}_x \left[g(x)^2 \text{Var}_W[f(X_t^x)] \right] \leq \tilde{\gamma}.$$

In the case where the $x_j = X_{jt}^{x_1}$, then for any $l \geq 1$ we have

$$(21) \quad \mathbb{E}_W \left[g(X_{lt}^{x_1})^2 \text{Var}[f(X_{(l+1)t}^{x_1})] \right] \leq \tilde{\gamma}.$$

If the basis functions are bounded, then (20) holds automatically. Note that (21) will be satisfied for an ergodic Markov chain with a stationary distribution μ for which (20) holds. In our numerical examples the basis functions are all bounded on \mathcal{M} .

PROPOSITION 2.6. *Fix $t > 0$ and the basis $\{\psi_1, \dots, \psi_N\}$, and let the assumptions of [Assumption 2.5](#) hold. Define $K_{\mu_T} = \frac{1}{T} (\mathcal{K}^t \psi(\mathbf{X})) \psi(\mathbf{X})^\top$ and $\hat{K}_T = \frac{1}{T} \psi(\mathbf{Y}) \psi(\mathbf{X})^\top$. Then, by taking expectations over the distributions of \mathbf{X} and \mathbf{Y} ,*

$$(22) \quad \mathbb{E}_{\mathbf{X}}[K_{\mu_T}] = \mathbb{E}_{\mathbf{X}, \mathbf{Y}}[\hat{K}_T].$$

Further, there exists a $\gamma > 0$ independent of T , such that

$$(23) \quad \mathbb{E}_{\mathbf{X}, \mathbf{Y}} \left\| K_{\mu_T} - \hat{K}_T \right\|_F^2 \leq \gamma T^{-1}.$$

Proof. We start by showing that (22) holds. First, note that the (i, j) th elements are given by

$$(24) \quad (\hat{K}_T)_{i,j} = \frac{1}{T} \sum_{k=1}^T \psi_i(y_k) \psi_j(x_k)$$

$$(25) \quad (K_{\mu_T})_{i,j} = \frac{1}{T} \sum_{k=1}^T \mathcal{K}^t \psi_i(x_k) \psi_j(x_k).$$

Let $f, g \in \{\psi_1, \dots, \psi_N\}$, and consider the following expectation with respect to the

distribution of (\mathbf{X}, \mathbf{Y}) .

$$(26) \quad \mathbb{E}_{\mathbf{X}, \mathbf{Y}} \left[\sum_{k=1}^T f(y_k)g(x_k) \right] = \sum_{k=1}^T \mathbb{E}_{x_k, y_k} [f(y_k)g(x_k)]$$

$$(27) \quad = \sum_{k=1}^T \mathbb{E}_{x_k} \left[\mathbb{E}_W [f(X_t^{x_k})]g(x_k) \right]$$

$$(28) \quad = \sum_{k=1}^T \mathbb{E}_{x_k} [\mathcal{K}^t f(x_k)g(x_k)]$$

$$(29) \quad = \mathbb{E}_{\mathbf{X}} \left[\sum_{k=1}^T \mathcal{K}^t f(x_k)g(x_k) \right].$$

The second line follows from the law of total expectations, and the third from the definition of the Koopman operator. It follows that $\mathbb{E}_{\mathbf{X}, \mathbf{Y}}(\hat{K}_T)_{i,j} = \mathbb{E}_{\mathbf{X}}(K_{\mu_T})_{i,j}$ for $i, j = 1, \dots, N$, which proves (22).

To prove the mean-square bound, we again consider $f, g \in \{\psi_1, \dots, \psi_N\}$. By linearity

$$(30) \quad \mathbb{E}_{\mathbf{X}, \mathbf{Y}} \left[\sum_{k=1}^T g(x_k) \{ \mathcal{K}^t f(x_k) - f(y_k) \} \right]^2 = \sum_{k=1}^T \mathbb{E}_{x_k, y_k} \left[g(x_k)^2 \{ \mathcal{K}^t f(x_k) - f(y_k) \}^2 \right]$$

$$(31) \quad + 2 \sum_{l < k} \mathbb{E}_{x_k, x_l, y_k, y_l} \left[g(x_k)g(x_l) \{ \mathcal{K}^t f(x_k) - f(y_k) \} \{ \mathcal{K}^t f(x_l) - f(y_l) \} \right].$$

All the terms in the second sum are zero. To see this, first note that, by the law of total expectations, each term in the sum are equal to

$$(32) \quad \mathbb{E}_{x_k, x_l, y_k} \left[g(x_k)g(x_l) \{ \mathcal{K}^t f(x_k) - f(y_k) \} \{ \mathcal{K}^t f(x_l) - \mathbb{E}_{y_l} [f(y_l)] \} \right].$$

Then, because $\mathbb{E}_{y_l} [f(y_l)] = \mathbb{E}_W [f(X_t^{x_l})] = \mathcal{K}^t f(x_l)$, it follows that the final bracket in (32) is zero. In a similar fashion we see that the terms in the first sum of (30) equal

$$(33) \quad \mathbb{E}_{x_k} \left[g(x_k)^2 \mathbb{E}_{y_k} \left(\mathbb{E}_{y_k} [f(y_k)] - f(y_k) \right)^2 \right] = \mathbb{E}_{x_k} \left[g(x_k)^2 \text{Var}_{y_k} [f(X_t^{x_k})] \right].$$

By [Assumption 2.5](#) this expectation is bounded by $\tilde{\gamma}$ for $k = 1, \dots, T$. We therefore have

$$(34) \quad \mathbb{E}_{\mathbf{X}, \mathbf{Y}} \left[\sum_{k=1}^T g(x_k) \{ \mathcal{K}^t f(x_k) - f(y_k) \} \right]^2 \leq \tilde{\gamma}T.$$

The result therefore follows by summing over all the N^2 entries of the matrices,

$$(35) \quad \mathbb{E}_{\mathbf{X}, \mathbf{Y}} \left\| K_{\mu_T} - \hat{K}_T \right\|_F^2 \leq \frac{N^2}{T^2} \tilde{\gamma}T = \gamma T^{-1},$$

where $\gamma = N^2 \tilde{\gamma}$. □

Using [Proposition 2.6](#) we finally state a result on how well the matrix representation of the EDMD operator approximates the Koopman operator.

COROLLARY 2.7. *Let the assumptions of Proposition 2.6 hold with bound constant γ , and further assume that the second moment of the mass matrix Frobenius norm is bounded above, that is*

$$(36) \quad \mathbb{E}_{\mathbf{X}} \|M_{\mu_T}^{-1}\|_F^2 \leq \tilde{M},$$

for some $\tilde{M} > 0$, independent of T .

Then the difference between the matrix representations of the EDMD and Koopman operators Koopman operator in the Frobenius norm is of order $T^{-1/2}$,

$$(37) \quad \mathbb{E}_{\mathbf{X}, \mathbf{Y}} \|A_{\mu_T} - \hat{A}_T\|_F \leq \sqrt{\frac{\gamma \tilde{M}}{T}}.$$

Proof. From Propositions 2.4 and 2.6 and their proofs we know that the matrix representations of the projected Koopman and EDMD operators are $A_{\mu_T} = K_{\mu_T} M_{\mu_T}^{-1}$ and $\hat{A}_T = \hat{K}_T M_{\mu_T}^{-1}$ respectively. Further, the Frobenius norm of a product is bounded by the product of the norms,

$$(38) \quad \|(K_{\mu_T} - \hat{K}_T) M_{\mu_T}^{-1}\|_F \leq \|K_{\mu_T} - \hat{K}_T\|_F \|M_{\mu_T}^{-1}\|_F.$$

By the Cauchy-Schwarz inequality,

$$(39) \quad \mathbb{E}_{\mathbf{X}, \mathbf{Y}} \left[\|K_{\mu_T} - \hat{K}_T\|_F \|M_{\mu_T}^{-1}\|_F \right] \leq \sqrt{\mathbb{E}_{\mathbf{X}, \mathbf{Y}} \|K_{\mu_T} - \hat{K}_T\|_F^2} \sqrt{\mathbb{E}_{\mathbf{X}, \mathbf{Y}} \|M_{\mu_T}^{-1}\|_F^2}.$$

The result now follows by applying (23) and (37) to the right hand side. \square

For completeness we note that the EDMD method can be adjusted to approximate the Perron–Frobenius operator by the matrix [14]

$$(40) \quad K_{\mu_T}^{\top} M_{\mu_T}^{-1}.$$

2.4. Parameter estimation using projected Koopman operators. In the following, we write $\mathcal{K}^t(\theta)$ when we want to emphasise the θ -dependence of the time- t Koopman operator. We will emphasise the θ -dependence in a similar fashion for the projected Koopman operators and their matrix representations, when needed.

Assume the output data \mathbf{Y} is generated from the SDE with a particular parameter θ^* and initial conditions \mathbf{X} . Then $\mathcal{K}_{\mu_T}^t(\theta^*) \approx \hat{\mathcal{K}}_T$, with equality whenever $b(x; \theta^*) \equiv 0$. Further, Corollary 2.7 motivates estimating θ^* by solving the minimisation problem

$$(41) \quad \min_{\theta \in \Theta} \|A_{\mu_T}(\theta) - \hat{A}_T\|_F^2.$$

We choose to minimise the Frobenius norm instead of the matrix norm induced by the inner product of G_{ψ} , because it is cheaper to calculate, and numerical investigations indicated similar performance. Further discussion on the formulation using matrix norms is given in Section 4.

Calculating the matrix $K_{\mu_T}(\theta)$ in $A_{\mu_T}(\theta) = K_{\mu_T}(\theta) M_{\mu_T}^{-1}$ requires the solution of the SDE, which in most cases would make this method intractable. We can, however, take advantage of the infinitesimal generator of the SDE to calculate $A_{\mu_T}(\theta)$ cheaply. In the remainder of the section, we define the infinitesimal generator, explain how it can be used to calculate $A_{\mu_T}(\theta)$, and summarise the parameter estimation method in Algorithm 1.

DEFINITION 2.8. *The continuous-time Koopman operator, \mathcal{K} , is the infinitesimal generator of the time- t Koopman operators,*

$$(42) \quad \mathcal{K}g(x) = \lim_{t \downarrow 0} \frac{\mathcal{K}^t g(x) - g(x)}{t}.$$

It is a well-known result that the continuous-time Koopman operator is a linear, second-order differential operator on well-behaved functions. See, for example, [3, Ch. 17] for a discussion and proof.

THEOREM 2.9. *Let $g \in C^2(\mathcal{M})$, then $\mathcal{K}(\theta) = \mathcal{L}(\theta)$, where*

$$(43) \quad \mathcal{L}(\theta)g(x) = \mathcal{L}[g(x); \theta] := a(x; \theta) \frac{dg(x)}{dx} + \frac{[b(x; \theta)]^2}{2} \frac{d^2g(x)}{dx^2}.$$

In the remainder of the section, we assume that the basis functions ψ_j are sufficiently smooth for (43) to hold on G_ψ . In addition, we require that G_ψ is invariant under $\mathcal{L}(\theta)$, that is, $\mathcal{L}(\theta)g \in G_\psi$ for all $g \in G_\psi$. The invariance assumption puts smoothness constraints on $a(x; \theta)$ and $b(x; \theta)$.

THEOREM 2.10. *Assume that $\mathcal{K} = \mathcal{L}$ on G_ψ , and that G_ψ is invariant under \mathcal{L} . Then $\mathcal{K}^t = e^{t\mathcal{K}}$ on G_ψ , and the matrix representation of \mathcal{K}_μ^t is given by*

$$(44) \quad A_\mu = \exp(tL_\mu M_\mu^{-1}),$$

where

$$(45) \quad L_\mu = \int_{\mathcal{M}} (\mathcal{L}\psi) \psi^\top d\mu.$$

Proof. The equality $\mathcal{K}^t = e^{t\mathcal{K}}$ on G_ψ follows from the definition of \mathcal{K} and the fact that linear operators are bounded on finite-dimensional spaces. This also means that this exponentiation relation holds for the matrix representations of \mathcal{K}^t and \mathcal{K} , with respect to a given inner product.

Following the same argument as in the proof of Theorem 2.3, we can show that

$$(46) \quad P_\psi^\mu \mathcal{L}g = c_g^\top L_\mu M_\mu^{-1} \psi, \quad \forall g = c_g^\top \psi \in G_\psi.$$

Since $P_\psi^\mu \mathcal{K} = P_\psi^\mu \mathcal{L}$ on G_ψ , their matrix representations are the same. It follows that the matrix representation A_μ of \mathcal{K}_μ^t is given by equation (44). \square

2.5. Proposed Algorithm. Algorithm 1 describes our SDE parameter estimation method, based on the minimisation problem (41), and Theorem 2.10. With a large number of basis functions, or when extending the method to higher-dimensional state spaces, calculating the projected Koopman and EDMD matrices may become expensive. Computationally efficient implementations of (extended) dynamic mode decomposition, based on SVD factorisations, can be used to alleviate such issues. See, for example, Tu *et. al.* [31] for an overview. In the numerical example of Subsection 3.1, however, we see that the algorithm performs as well as existing SDE parameterisation methods already with three basis functions.

Remark 2.11. If $\mathcal{L}(\theta)$ is linear in the parameters, one can pre-calculate the integrals of the matrix $L(\theta)$ in Algorithm 1 such that each function evaluation of the minimisation problem is reduced to scalar-matrix and matrix exponentiation operations. We take advantage of this for our examples in Section 3.

Algorithm 1 EDMD parameter estimation

Require: Data $\mathbf{X} = [x_1, \dots, x_T]$, $\mathbf{Y} = [y_1, \dots, y_T]$, and time-step $t > 0$

Require: Basis functions $\boldsymbol{\psi}(x) = [\psi_1(x), \dots, \psi_N(x)]^\top$

Require: Infinitesimal generator $\mathcal{L}(\theta) = a(x; \theta) \frac{d}{dx} + \frac{1}{2} b(x; \theta)^2 \frac{d^2}{dx^2}$

- 1: Set $M \leftarrow \frac{1}{T} \boldsymbol{\psi}(\mathbf{X}) \boldsymbol{\psi}(\mathbf{X})^\top$
- 2: Set $A \leftarrow \frac{1}{T} \boldsymbol{\psi}(\mathbf{Y}) \boldsymbol{\psi}(\mathbf{X})^\top M^{-1}$
- 3: Define $\mu(x) = \frac{1}{T} \sum_{j=1}^T \delta(x - x_j)$
- 4: Define $L(\theta) = \int_{\mathcal{M}} (\mathcal{L}(\theta) \boldsymbol{\psi}) \boldsymbol{\psi}^\top d\mu$
- 5: Solve

$$\hat{\theta} = \arg \min_{\theta \in \Theta} \left\| \exp(tL(\theta)M^{-1}) - A \right\|_F^2.$$

6: **return** $\hat{\theta}$

Remark 2.12. The theoretical motivation for the algorithm assumed that $G_{\boldsymbol{\psi}}$ was invariant under \mathcal{L} . Our choices of basis functions in the numerical examples do not necessarily satisfy this assumption.

Remark 2.13. Instead of matching the exponential matrix $\exp(tL(\theta)M^{-1})$ to the EDMD matrix A in step five, one can match $L(\theta)M^{-1}$ to a branch of the matrix logarithm $\log(A)/t$. As noted by [20, 21], it is not clear which branch of the matrix logarithm to choose if we follow this approach.

3. Numerical Examples.

3.1. The Ornstein–Uhlenbeck Process. In this section we compare the performance of the proposed EDMD-based parameter estimation algorithm to existing methods. The numerical example and data is taken from Hurn *et. al.* [12], where the authors compare the performance of 14 different SDE parameter estimation algorithms. The data from the comparison paper is available at <http://www.ncer.edu.au/resources/data-and-code.php>. The Ornstein-Uhlenbeck equation is the SDE

$$(47) \quad dX_t = \theta_1(\theta_2 - X_t) dt + \theta_3 dW_t.$$

The infinitesimal generator of solutions to this SDE is

$$(48) \quad \mathcal{L}(\theta) = \theta_1(\theta_2 - x) \frac{d}{dx} + \frac{\theta_3^2}{2} \frac{d^2}{dx^2}.$$

Note that evaluation of the matrix $L_\mu(\theta)$ can be very cheap, by pre-calculating the integrals involved:

$$(49) \quad L_\mu(\theta) = \theta_1 \theta_2 \int_{\mathcal{M}} \frac{d\boldsymbol{\psi}(x)}{dx} \boldsymbol{\psi}(x)^\top d\mu(x) - \theta_1 \int_{\mathcal{M}} x \frac{d\boldsymbol{\psi}(x)}{dx} \boldsymbol{\psi}(x)^\top d\mu(x) + \frac{\theta_3^2}{2} \int_{\mathcal{M}} \frac{d^2\boldsymbol{\psi}(x)}{dx^2} \boldsymbol{\psi}(x)^\top d\mu(x).$$

Then, subsequent evaluations of $L_\mu(\theta)$ are simply scalar-matrix computations.

The data set from [12] consists of 2000 independent sample paths with 501 data points each, separated with a time step $\Delta t = 1/12$. They are all drawn from the SDE

with parameter $\theta^* = (0.2, 0.08, 0.03)$. For each sample path, we employ [Algorithm 1](#) to estimate θ^* . For this example, we test the performance of radial basis functions (RBFs) of the form

$$(50) \quad \psi_j(x) = \exp \left\{ -l^2(x - c_j)^2 \right\}, \quad j = 1, \dots, N,$$

where $l > 0$ is a given length scale, and c_j an increasing sequence of centre points. With N basis functions, the centre points are chosen to be spaced at a distance $\Delta x_N > 0$ apart, so that $c_1 = \min\{\mathbf{X}\} + \Delta x_N$ and $c_N = \max\{\mathbf{X}\} - \Delta x_N$. The length scale is set to $l = 1/\Delta x_N$. The parameter estimation is done with $N = 3, 4, 5$. In [Figure 1](#), the basis functions, when $N = 3$, are shown for the first sample path in the data set.

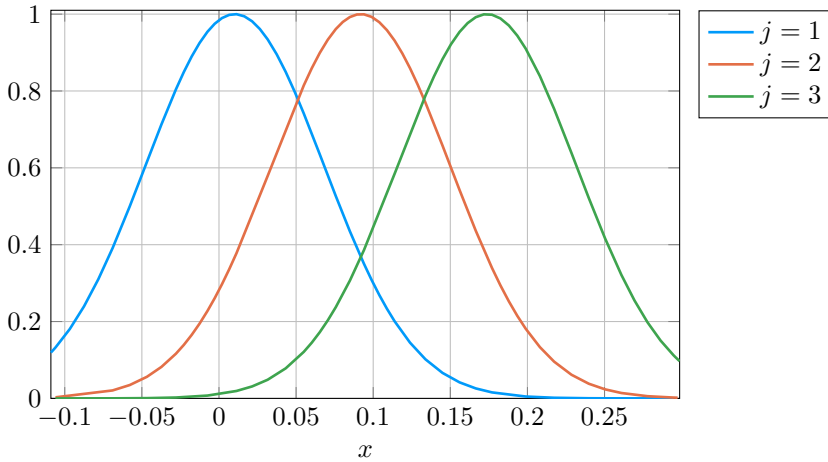


Fig. 1: The RBFs $\psi_j(x)$ for $N = 3$, with centre points and length scale calculated based on the first sample path in the data set.

Remark 3.1. The basis functions depend on the data, which is not consistent with the assumptions of [Proposition 2.6](#) and [Corollary 2.7](#). We note, however, that as T increases, the probability that $\max\{\mathbf{X}\}$ and $\min\{\mathbf{X}\}$ varies becomes small. One can also restrict the c_j to be within a box, so that eventually the basis functions stay fixed.

The minimisation step uses the BFGS algorithm [23], with interpolation backtracking, implemented by the `Optim.jl` package [22] in the Julia programming language [1]. Derivatives are calculated using finite differences. The initial guess is set to θ^* , to be consistent with the comparisons done in Hurn *et. al.* [12]. Numerical investigations, not included here, show that the objective function is convex for the different data sets.

In [Table 1](#), statistics of the performance of the algorithm for $N = 3, 4, 5$ is presented. For a few of the 2000 sample paths, the algorithm estimation is far off the correct parameter θ^* , reporting $|\hat{\theta}_2|$ to be orders of magnitude too large. These are typically sample paths for which the data predominantly stays on one side of the long-term mean θ_2^* , so that the mean-reversion property of the process is less apparent. We exclude these paths from the calculation of the statistics, and instead report any values where $|\hat{\theta}_j| > 1$, for at least one of $j = 1, 2, 3$, as failures. Let $\theta^{k,*}$ denote the reported parameter for the k^{th} sample path. The table shows the bias and root mean

squared (RMS) values for the estimates, which are calculated as $\frac{1}{T} \sum_{k=1}^{2000} (\theta_j^{k,*} - \theta_j^*)$ and $\sqrt{\frac{1}{T} \sum_{k=1}^{2000} (\theta_j^{k,*} - \theta_j^*)^2}$ respectively. These values are compared to the results from the exact maximum likelihood (EML) reference algorithm used in Hurn *et. al.* [12]. Note that parameter estimation with EML is only available if one knows the transition probability density of the associated SDE. The other 13 algorithms reported very similar performance statistics. From the table, we can see that our proposed algorithm performs just as well as the reference EML algorithm.

Alg	θ_1		θ_2		θ_3		Fail
	Bias	RMSE	Bias	RMSE	Bias	RMSE	
RBF(3)	0.0850	0.1748	-0.0014	0.0317	-0.0000	0.0023	7
RBF(4)	0.0860	0.1880	-0.0020	0.0428	0.0002	0.0019	22
RBF(5)	0.0908	0.1874	-0.0007	0.0372	0.0003	0.0017	19
EML	0.1101	0.1780	-0.0006	0.0227	0.0001	0.0010	—

Table 1: Performance statistics comparing [Algorithm 1](#) with different number of RBFs. The row with the EML results are taken from [12].

3.1.1. Performance with increasing amount of data. We end the Ornstein-Uhlenbeck example by investigating the estimation improvement with increasing amount of data T while keeping the time step fixed. [Corollary 2.7](#) suggests that the EDMD matrix will better approximate the projected Koopman matrix as T increases. To this end, we created 2000 sample paths of the solution to (47), with $\theta^* = (0.2, 0.08, 0.03)$, all started at the initial condition $X_0 = \theta_2 = 0.08$. The data is stored at time steps $\Delta t = 1/12$ apart, and generated from the exact conditional distribution given by

$$(51) \quad X_t^x \sim \mathcal{N}(\theta_2 + (x - \theta_2)e^{-\theta_1 t}, \theta_3^2 (1 - e^{-2\theta_1 t}) / 2\theta_1),$$

so that $x_{j+1} = X_{\Delta t}^{x_j}$ and $y_j = x_{j+1}$ for $j = 1, \dots, T-1$. [Figure 2](#) reports the root mean squared error of the estimators, with data amount $T = 500 \times 2^j$, for $j = 0, 1, \dots, 9$. We use RBFs calculated in the same way as in [Subsection 3.1](#), with $N = 3, 5, 10$. The number of failures are zero for the larger amounts of data, in particular no estimations are considered a failure for $N = 3$ and $j \geq 1$. The RMSE for θ_1 , and θ_2 decreases with data of order $\mathcal{O}(T^{-1/2})$, and the RMSE for θ_3 decreases approximately as $\mathcal{O}(T^{-1/3})$.

3.2. Bounded Mean Reversion Process. In [Subsection 3.1](#), we saw that our algorithm performs comparably well to other methods from the literature. Within the study of EDMD, a common theme is the calculation of eigenfunctions (related to left eigenvectors of the EDMD matrix) to examine the types of behaviour of the system. For systems with many timescales, or those that are confined to a low dimensional manifold, the eigenfunctions can be used to offer a low dimensional description of the system.

For a matrix A in the minimisation problem in equation (41) with ordered eigenvalues $1 = \lambda_1 > |\lambda_2| > \dots > |\lambda_N|$, and left and right eigenvectors (denoted \mathbf{w} and \mathbf{v}), then we can write the J -eigendecomposition of A as

$$(52) \quad A_J = \sum_{j=1}^J \lambda_j \mathbf{v}_j \mathbf{w}_j^T,$$

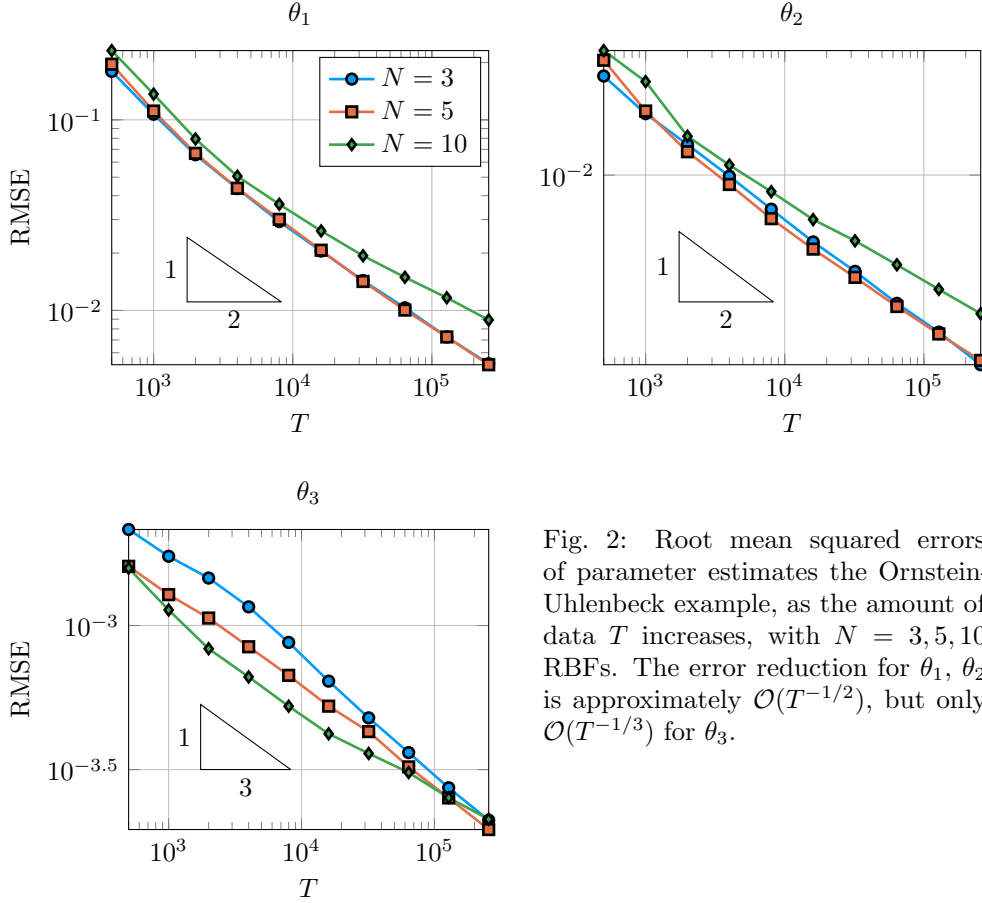


Fig. 2: Root mean squared errors of parameter estimates the Ornstein-Uhlenbeck example, as the amount of data T increases, with $N = 3, 5, 10$ RBFs. The error reduction for θ_1, θ_2 is approximately $\mathcal{O}(T^{-1/2})$, but only $\mathcal{O}(T^{-1/3})$ for θ_3 .

and $A_J = A$ when $J = N$. We then consider replacing A by A_J in equation (41) for varying J and N . We can interpret N as a parameter that controls the possible resolution of the data, and J the parameter that specifies the maximum allowed resolution in the generator.

To avoid numerical artefacts regarding sampling of data, we have devised a numerical experiment where: we use a large amount of data points; and we vary the types of basis functions used by considering global basis functions, and deterministically placed RBFs (rather than depending on the range of a sample path as in Subsection 3.1). We consider the SDE with parameters $\theta = (\theta_1, \theta_2)$

$$(53) \quad dX_t = -2\theta_1 X_t dt + \sqrt{2\theta_2(1 - X_t^2)} dW_t,$$

which is a mean reversion process (to $x = 0$) bounded on the interval $(-1, 1)$. The SDE given by equation (53) has infinitesimal generator

$$(54) \quad \mathcal{L}(\theta) = \theta_2(1 - x^2) \frac{d^2}{dx^2} - 2\theta_1 x \frac{d}{dx}.$$

Similar to in Subsection 3.1, the matrix $L_\mu(\theta)$ can be pre-calculated. We then consider the following basis functions

1. Chebychev polynomials, defined on $[-1, 1]$ as

$$(55) \quad \begin{aligned} T_0(x) &= 1, \\ T_1(x) &= x, \\ T_{n+1}(x) &= 2xT_n(x) - T_{n-1}(x), \end{aligned}$$

and then $\psi_j = T_{j-1}$ for $j = 1 \dots N$.

2. Gaussian RBFs as given by equation (50). We position each basis equally along the interval $[-1, 1]$ so $c_j = -1 + 2(j-1)/(N-1)$ and choose the scaling constant to be the distance between points, $l = 2/(N-1)$.
3. Legendre polynomials, defined on $[-1, 1]$ as

$$(56) \quad \begin{aligned} P_0(x) &= 1, \\ P_1(x) &= x, \\ (n+1)P_{n+1}(x) &= (2n+1)xP_n(x) - nP_{n-1}(x), \end{aligned}$$

and then $\psi_j = P_{j-1}$ for $j = 1 \dots N$.

This choice was made as Chebychev polynomials are a popular choice for polynomial basis functions on bounded intervals; RBFs offer customisable ways of spanning a domain (with a multitude of methods choosing the centre locations); and Legendre polynomials are the eigenfunctions of the infinitesimal generator when $\theta^* = (1, 1)$.

In [Figure 3](#) we show a comparison between the different basis functions to estimate $\theta^* = (1, 1)$ for different numbers of basis functions N and different numbers of eigenfunctions in the eigen-expansion $J \leq N$. The simulation was set up with a very large number of data points, we sample for 1000 time units using the Milstein method with a time step of $\Delta t = 2^{-12}$. For the Chebychev and Legendre polynomials $2 \leq J \leq N \leq 46$, and for the RBFs $4 \leq J \leq N \leq 92$.

From [Figure 3](#), when $N = J$ we find that Chebychev polynomials estimate the parameters well for all N — we note that in [Figure 3](#), it is not always possible to see this effect for small N . For larger values of N we notice two trends: first, as we add extra basis functions the estimates do not change; second, it is not always necessary to have $J = N$ and one can occasionally obtain a better estimate with $J < N$. One interpretation of this is that with small N , every eigenfunction is important; however there is error in the data set (generated by the Milstein SDE numerical scheme), and this error may manifest itself in the higher order modes, so it can be beneficial to exclude them. Finding the exact point at which to truncate is not immediately obvious.

We now consider the radial basis function results in [Figure 3](#). One thing to note about RBFs is that the locations and scaling parameters have change as N varies. Therefore, one has to be careful when comparing the system with N basis functions to the system with $N + 1$ basis functions. This manifests itself in [Figure 3](#) as a non-monotonic behaviour for large N, J . The general trend however is that increasing the number of basis functions improves the accuracy of the estimate, and one should use the full eigen-expansion with $J = N$.

Finally, the Legendre polynomial plots in [Figure 3](#) appear similarly to the Chebychev polynomial plots. We also get the highest accuracy of parameter estimation, however we are using *a priori* information in that we know the correct eigenfunctions.

4. Variations of the algorithm. In this section we discuss variations of the algorithm with different choices of objective. In particular, using the operator norm,

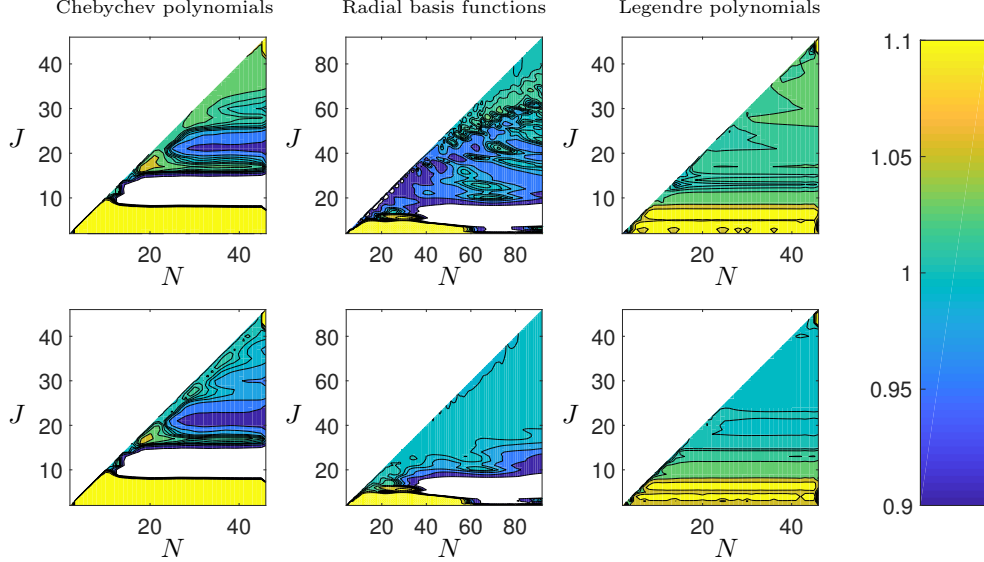


Fig. 3: Estimate plots for parameters $\theta_1 = 1$ (top row) and $\theta_2 = 1$ (bottom row) when varying N and J . The underlying data set is generated from a single sample path of equation (53) simulated using the Milstein method for 1000 time units with $\Delta t = 2^{-12}$. Estimates in the range $(0.9, 1.1)$ are plotted in colour, estimates outside this range (including when $J > N$) are in white. The contour lines are at $1 \pm 2^{-n}/10$ for $n = 0, 1, 2, 3, 4$.

constrained EDMD, and generalised method of moments [9]. In numerical tests, not all included in this article, we find that all the methods have a (sometimes significantly) larger function evaluation cost, without major improvements to the parameter estimates.

In addition to the variations covered in this section, note that operator matching of the Perron–Frobenius operator under the operator or Frobenius norms can be done in similar ways. It follows by considering the Perron–Frobenius matrix $K_{\mu_T}^T M_{\mu_T}^{-1}$ from (40), and the similarly defined data-driven matrix.

4.1. Operator norm. In Subsection 2.4 and for our proposed algorithm, we try to match the projected Koopman operator $\mathcal{K}_{\mu_T}^t(\theta)$ to the EDMD operator $\hat{\mathcal{K}}_T$ by minimising the distance between their matrix representations under the Frobenius norm. Another natural choice would be to match the two operators under the operator norm induced by the inner product on G_ψ . For a linear operator $\mathcal{A} : G_\psi \rightarrow G_\psi$, the operator norm with respect to the $L^2(\mu_T)$ inner product is given by

$$(57) \quad \|\mathcal{A}\|_{\mu_T} = \sup_{g \neq 0} \sqrt{\frac{\int_{\mathcal{M}} [\mathcal{A}g(x)]^2 d\mu_T(x)}{\int_{\mathcal{M}} [g(x)]^2 d\mu_T(x)}}.$$

Likewise, for a matrix $A \in \mathbb{R}^{N \times N}$, the matrix norm with respect to the ℓ_2 inner product on \mathbb{R}^N , weighted by a positive definite matrix $M \in \mathbb{R}^{N \times N}$, is given by

$$(58) \quad \|A\|_M = \sup_{c \neq 0} \sqrt{\frac{c^T A^T M A c}{c^T M c}}.$$

As G_ψ is finite dimensional, \mathcal{A} has a matrix representation A in the basis ψ , such that $\mathcal{A}g = c_g^\top A \psi$. Thus, the operator norm reduces to

$$(59) \quad \|\mathcal{A}\|_{\mu_T} = \sup_{c_g \neq 0} \sqrt{\frac{c_g^\top A \left(\int_{\mu} \psi \psi^\top d\mu_T \right) A^\top c_g}{c_g^\top \left(\int_{\mu} \psi \psi^\top d\mu_T \right) c_g}} = \|A^\top\|_{M_{\mu_T}} = \|A\|_{M_{\mu_T}},$$

where the norm of A in equation (59) is equal to its transpose as the mass matrix is symmetric. For the projected Koopman and EDMD operators, we thus have

$$(60) \quad \left\| \mathcal{K}_{\mu_T}^t(\theta) - \hat{\mathcal{K}}_T \right\|_{\mu_T} = \left\| A_{\mu_T}(\theta) - \hat{A}_T \right\|_{M_{\mu_T}}.$$

Thus, a potentially more natural approach than minimising the Frobenius norm in (41) and Algorithm 1 could be find the solution to the minimisation problem

$$(61) \quad \min_{\theta \in \Theta} \left\| A_{\mu_T}(\theta) - \hat{A}_T \right\|_{M_{\mu_T}}.$$

Objective evaluations of (61) are more expensive than the Frobenius norm, however it does not yield any better parameter estimates: We have compared the two methods for the numerical experiments in this article, and neither method particularly dominates the other.

4.2. Constrained EDMD. Instead of calculating the EDMD operator and matching the Koopman operator against that, we could also try to do parameter estimation by constraining the EDMD matrix minimisation in (6) so that the matrix A is of the form $A_{\mu_T} = \exp(tL_{\mu_T}M_{\mu_T}^{-1})$. This yields the optimisation problem

$$(62) \quad \min_{\theta \in \Theta} \|A_{\mu_T}(\theta)\psi(\mathbf{X}) - \psi(\mathbf{Y})\|_F^2 = \min_{\theta \in \Theta} \sum_{j=1}^T \|A_{\mu_T}(\theta)\psi(x_j) - \psi(y_j)\|_2^2.$$

The number of floating point operations required to evaluate this norm grows linearly with the amount of data, and hence it becomes expensive to perform parameter estimation with large amounts of data. To compare, in our proposed algorithm, the evaluation of the norm is independent of data size.

To be sure, constrained EDMD parameter estimation with the objective (62), can provide good results. In Table 2, we provide convergence statistics that compares Algorithm 1 with constrained EDMD. The table reports the root mean squared error with three RBFs, from the 2000 Ornstein-Uhlenbeck sample paths from Subsection 3.1.1. The parameter estimates are slightly better for constrained EDMD, and in particular it improves the convergence rate for θ_3 : The error decreases at approximately $\mathcal{O}(T^{-1/2})$, compared to approximately $\mathcal{O}(T^{-1/3})$ with Algorithm 1.

The improvements come at a cost, however. First, the objective in (62) results in ill-conditioning for the backtracking line search with BFGS and the optimiser diverges. To prevent this, we had to employ the more costly line search by Hager and Zhang [7], which requires more gradient evaluations. Second, evaluating the objective and gradients are more expensive, especially for larger amounts of data. Users of the algorithms should choose between these objectives based on their computational budget and amount of data.

j	θ_1		θ_2		θ_3	
	Alg 1	C-EDMD	Alg 1	C-EDMD	Alg 1	C-EDMD
0	1.795	1.654	3.042	3.315	2.154	1.785
1	1.070	0.983	1.976	1.767	1.739	1.282
2	0.656	0.610	1.403	1.216	1.461	0.946
3	0.436	0.417	0.987	0.840	1.161	0.662
4	0.293	0.282	0.685	0.586	0.874	0.459
5	0.205	0.196	0.476	0.407	0.641	0.323
6	0.143	0.137	0.344	0.293	0.478	0.233
7	0.103	0.097	0.241	0.209	0.362	0.175
8	0.053	0.046	0.122	0.102	0.211	0.089
	$\times 10^{-1}$	$\times 10^{-1}$	$\times 10^{-2}$	$\times 10^{-2}$	$\times 10^{-3}$	$\times 10^{-3}$

Table 2: Root mean squared error comparing the proposed [Algorithm 1](#) to constrained EDMD (62) for $T = 500 \times 2^j$ data points. The results are reported from 2000 sample paths of the OU process in [Subsection 3.1.1](#), with three RBFs as explained in the OU process example.

4.3. Generalised method of moments. The method of moments approach to parameter estimation is based on the knowledge of relationships between parameters of a random variable and its moments. For example, the mean and variance parameters of a Gaussian random variable can be matched to the empirical mean variance from a collection of data. One can further extend this idea to match the expected value and empirical mean of arbitrary functions defined on the output space of a random variable [9]. We take advantage of the Koopman operator to match expected values to empirical means using the basis functions of G_ψ . The approach is similar to constrained EDMD, however the sum over data is taken inside the chosen norm on \mathbb{R}^N , as opposed to summing over the norm in (62).

Let x_0 be a random variable distributed according to some underlying probability space $(\mathcal{M}, \mathcal{B}, \mu)$. For a fixed $t > 0$, define $Y = X_t^{x_0}$, a random variable induced by the product measure of the Brownian motion and μ . For $g \in \mathcal{G}$, the expected value of $g(Y)$ is given by

$$(63) \quad \mathbb{E}[g(Y)] = \int_{\mathcal{M}} \mathbb{E}_W [g(X_t^x)] d\mu(x) = \int_{\mathcal{M}} \mathcal{K}^t(\theta)g(x) d\mu(x).$$

The method of moments aims to find $\theta \in \Theta$ to match the expected value of $g(Y)$ for functions $g \in \mathcal{G}$ with the sample mean $m_g = \frac{1}{T} \sum_{j=1}^T g(y_j)$. For a vector field $\mathbf{g} = (g_1, \dots, g_r) \in \mathcal{G}^r$, define the vector sample mean $\mathbf{m}_g = [m_{g_1}, \dots, m_{g_r}]$. The generalised method of moments is then defined as finding a solution to

$$(64) \quad \theta^* = \arg \min_{\theta \in \Theta} \|\mathbb{E}[\mathbf{g}(Y)] - \mathbf{m}_g\|,$$

for a choice of norm on \mathbb{R}^r .

Now, choose $\mu = \mu_T$, and let $\mathbf{g} = \psi \in G_\psi^N$. Then, $\mathcal{K}^t(\theta)\mathbf{g}(x) = A_{\mu_T}(\theta)\psi(x)$. We see from (63) that

$$(65) \quad \mathbb{E}[\mathbf{g}(Y)] = \int_{\mu_T} A_{\mu_T}(\theta)\psi(x) d\mu_T(x) = \frac{1}{T} \sum_{j=1}^T A_{\mu_T}(\theta)\psi(x_j).$$

If we choose the ℓ_2 norm on \mathbb{R}^N , then the method of moments minimisation (64) becomes

$$(66) \quad \theta^* = \arg \min_{\theta \in \Theta} \left\| \frac{1}{T} \sum_{j=1}^T A_{\mu_T}(\theta) \psi(x_j) - \psi(y_j) \right\|_2.$$

Contrast (66) to the constrained EDMD problem (62): The sum over data is taken inside the norm.

In numerical tests, generalised method of moments with the ℓ_2 -norm gives a very poor estimation performance, and function evaluations become expensive as the amount of data increases. The first point can potentially be fixed, by changing the inner product on \mathbb{R}^N to be an Σ^{-1} -weighted ℓ_2 inner product. The most effective choice of the inverse weighting matrix Σ is, according to [9, 12], given by

$$(67) \quad \Sigma_{i,j} = \frac{1}{T} \sum_{k=1}^T ([A_{\mu_T}(\theta^*) \psi_i(x_k) - \psi_i(y_k)][A_{\mu_T}(\theta^*) \psi_j(x_k) - \psi_j(y_k)]).$$

As we do not know θ^* in advance, this becomes an iterative procedure in estimating Σ and performing the optimisation.

5. Discussion and Conclusion. In this paper, we presented a method to parameterise SDEs based off approximating the generator. We provided bounds on the mean square error of the EDMD matrix as an estimator in Section 2, numerical examples in Section 3, and suggested variations to the method in Section 4. Thus far, our work has been limited to SDEs, although other models are also of interest. We envision our method being a suitable starting point to parameterising a wide range of stochastic dynamical systems when the generator of the process is known. The methodology could also be applied to deterministic systems, although more established methodologies already exist (e.g., minimising mean squared error).

Our algorithm appears to not fit into the broad MLE or MM categories for parameter estimation. Therefore, our work opens up new research directions which we now briefly discuss.

One of the advantages to our method is that once the data matrices $\psi(\mathbf{X})$ and $\psi(\mathbf{Y})$ are constructed, the parameter search does not depend on the number of data points T , only the number of basis functions N . In the limit of large data $T \gg N$, the data matrices will be computationally intensive to construct, so we hope to sub-sample the data and compute these efficiently. Additionally, there are alternatives to Monte Carlo sampling of the generator matrix L_μ . For example, one could use kernel density estimation to find μ , and use numerical integration to calculate the matrix entries.

Numerical experiments show that the method performs as well as a wide range of existing methods. In Subsection 3.1.1 we find that the convergence rate of the parameter estimation errors decrease by orders $\mathcal{O}(T^{-1/2})$ and $\mathcal{O}(T^{-1/3})$, perhaps indicating that accelerating ideas from Monte Carlo approximations can improve convergence. In the numerical example in Subsection 3.2, we investigated prediction accuracy whilst varying numbers of basis functions and numbers of eigenfunctions in the approximation. Occasionally it was the case that a limited eigen-expansions of the Koopman operator was preferable to the full matrix. It is not clear when a limited eigen-expansion is preferable to the full matrix.

When considering models with many parameters, there are many issues around the topics of model selection, confidence in parameters, and sensitivity analysis [8, 13, 34].

This is especially the case in our work when many SDEs correspond to the same infinitesimal generator⁴ [30]. Theoretical advancements relating to rates of convergence, especially with regards to error analysis, are now of critical importance to promote the use of our method. We also see the need to test our method on high dimensional stochastic dynamical systems, especially ones in which diverse ranges of behaviour are possible.

Contributions. J.P.T-K and A.N.R contributed equally to this article. J.P.T-K had the idea of EDMD-based parameter estimation, and performed the numerical experiments with lower order eigenfunction expansions. A.N.R devised the proposed algorithm and the theoretical connection to Koopman theory, performed the numerical experiments on the OU process, and formalised the variations of the algorithm.

Acknowledgements. A.N.R and J.P.T-K both received funding from the EPSRC under grant reference numbers EP/L015803/1 (A.N.R), and EP/G037280/1 (J.P.T-K). We thank Stefan Klus, Péter Koltai, Scott Dawson, and in particular Tomislav Plesa, for helpful discussions.

References.

- [1] J. BEZANSON, A. EDELMAN, S. KARPINSKI, AND V. B. SHAH, *Julia: A fresh approach to numerical computing*, SIAM Review, 59 (2017), pp. 65–98.
- [2] H. G. BOCK, E. KOSTINA, AND J. P. SCHLÖDER, *Numerical methods for parameter estimation in nonlinear differential algebraic equations*, GAMM-Mitteilungen, 30 (2007), pp. 376–408.
- [3] S. COHEN AND R. J. ELLIOTT, *Stochastic calculus and applications*, Birkhäuser, 2 ed., 2015.
- [4] R. ERBAN, J. CHAPMAN, AND P. MAINI, *A practical guide to stochastic simulations of reaction-diffusion processes*, arXiv preprint arXiv:0704.1908, (2007).
- [5] C. W. GARDINER, *Handbook of stochastic methods for physics, chemistry and the natural sciences*, Springer-Verlag, 1994.
- [6] A. GOLIGHTLY AND D. J. WILKINSON, *Bayesian parameter inference for stochastic biochemical network models using particle Markov chain Monte Carlo*, Interface focus, 1 (2011), pp. 807–820.
- [7] W. W. HAGER AND H. ZHANG, *Algorithm 851: CG_DESCENT, a conjugate gradient method with guaranteed descent*, ACM Transactions on Mathematical Software (TOMS), 32 (2006), pp. 113–137.
- [8] D. HAMBY, *A review of techniques for parameter sensitivity analysis of environmental models*, Environmental monitoring and assessment, 32 (1994), pp. 135–154.
- [9] L. P. HANSEN, *Large sample properties of generalized method of moments estimators*, Econometrica: Journal of the Econometric Society, (1982), pp. 1029–1054.
- [10] F. HARTIG, J. M. CALABRESE, B. REINEKING, T. WIEGAND, AND A. HUTH, *Statistical inference for stochastic simulation models — theory and application*, Ecology letters, 14 (2011), pp. 816–827.
- [11] K. E. HINES, *A primer on Bayesian inference for biophysical systems*, Biophysical journal, 108 (2015), pp. 2103–2113.
- [12] A. S. HURN, J. JEISMAN, AND K. A. LINDSAY, *Seeing the wood for the trees: A critical evaluation of methods to estimate the parameters of stochastic differential equations*, Journal of Financial Econometrics, 5 (2007), pp. 390–455.
- [13] J. B. KADANE AND N. A. LAZAR, *Methods and criteria for model selection*, Journal of the American statistical Association, 99 (2004), pp. 279–290.

⁴This non-uniqueness arises from SDEs with multiple noise terms.

- [14] S. KLUS, P. KOLTAI, AND C. SCHÜTTE, *On the numerical approximation of the Perron-Frobenius and Koopman operator*, Journal of Computational Dynamics, 3 (2016), pp. 51–79, <https://doi.org/10.3934/jcd.2016003>, <http://aimsciences.org/journals/displayArticlesnew.jsp?paperID=12983>.
- [15] S. KLUS, F. NÜSKE, P. KOLTAI, H. WU, I. KEVREKIDIS, C. SCHÜTTE, AND F. NOÉ, *Data-driven model reduction and transfer operator approximation*, arXiv preprint arXiv:1703.10112, (2017).
- [16] B. O. KOOPMAN, *Hamiltonian systems and transformation in hilbert space*, Proceedings of the National Academy of Sciences, 17 (1931), pp. 315–318.
- [17] M. KORDA AND I. MEZIĆ, *On convergence of Extended Dynamic Mode Decomposition to the Koopman operator*, Journal of Nonlinear Science, 28 (2018), pp. 687–710, <https://doi.org/10.1007/s00332-017-9423-0>, <https://doi.org/10.1007/s00332-017-9423-0>.
- [18] J. N. KUTZ, S. L. BRUNTON, B. W. BRUNTON, AND J. L. PROCTOR, *Dynamic Mode Decomposition: Data-Driven Modeling of Complex Systems*, SIAM, 2016.
- [19] A. LASOTA AND M. C. MACKEY, *Probabilistic properties of deterministic systems*, Cambridge University Press, 1985.
- [20] A. MAUROY AND J. GONCALVES, *Linear identification of nonlinear systems: A lifting technique based on the koopman operator*, in Decision and Control (CDC), 2016 IEEE 55th Conference on, IEEE, 2016, pp. 6500–6505.
- [21] A. MAUROY AND J. GONCALVES, *Koopman-based lifting techniques for nonlinear systems identification*, ArXiv e-prints, (2017), <https://arxiv.org/abs/1709.02003>.
- [22] P. K. MOGENSEN AND A. N. RISETH, *Optim: A mathematical optimization package for Julia*, Journal of Open Source Software, 3 (2018), p. 615, <https://doi.org/10.21105/joss.00615>.
- [23] J. NOCEDAL AND S. J. WRIGHT, *Numerical optimization, second edition*, Numerical optimization, (2006), pp. 497–528.
- [24] G. A. PAVLIOTIS, *Stochastic processes and applications*, Springer, 2016.
- [25] M. PEIFER AND J. TIMMER, *Parameter estimation in ordinary differential equations for biochemical processes using the method of multiple shooting*, IET Systems Biology, 1 (2007), pp. 78–88.
- [26] R. PENROSE, *A generalized inverse for matrices*, Mathematical proceedings of the Cambridge philosophical society, 51 (1955), pp. 406–413, <https://doi.org/10.1017/S0305004100030401>.
- [27] U. PICCHINI, *Inference for SDE models via approximate Bayesian computation*, Journal of Computational and Graphical Statistics, 23 (2014), pp. 1080–1100.
- [28] J. O. RAMSAY, G. HOOKER, D. CAMPBELL, AND J. CAO, *Parameter estimation for differential equations: A generalized smoothing approach*, Journal of the Royal Statistical Society: Series B (Statistical Methodology), 69 (2007), pp. 741–796.
- [29] C. W. ROWLEY, I. MEZIĆ, S. BAGHERI, P. SCHLATTER, AND D. S. HENNINGSON, *Spectral analysis of nonlinear flows*, Journal of fluid mechanics, 641 (2009), pp. 115–127.
- [30] D. SCHNOERR, G. SANGUINETTI, AND R. GRIMA, *The complex chemical Langevin equation*, The Journal of chemical physics, 141 (2014), p. 07B606_1.
- [31] J. H. TU, C. W. ROWLEY, D. M. LUCHTENBURG, S. L. BRUNTON, AND J. N. KUTZ, *On Dynamic Mode Decomposition: Theory and applications*, Journal of Computational Dynamics, 1 (2014), pp. 391–421.
- [32] N. G. VAN KAMPEN, *Stochastic processes in physics and chemistry*, vol. 1, Elsevier, 1992.
- [33] M. O. WILLIAMS, I. G. KEVREKIDIS, AND C. W. ROWLEY, *A data-driven*

- approximation of the Koopman operator: Extending dynamic mode decomposition*, Journal of Nonlinear Science, 25 (2015), pp. 1307–1346.
- [34] X. ZHANG, J. CAO, AND R. J. CARROLL, *On the selection of ordinary differential equation models with application to predator-prey dynamical models*, Biometrics, 71 (2015), pp. 131–138.